

Dispersion engineered As₂S₃ planar waveguides for broadband four-wave mixing based wavelength conversion of 40 Gb/s signals

Feng Luan,¹ Mark D. Pelusi,¹ Michael R.E. Lamont,¹ Duk-Yong Choi,² Steve Madden,² Barry Luther-Davies,² and Benjamin J. Eggleton¹

¹Centre for Ultrahigh-bandwidth Devices for Optical Systems (CUDOS), IPOS, School of Physics, University of Sydney, NSW 2006, Australia

egg@physics.usyd.edu.au

²Centre for Ultrahigh-bandwidth Devices for Optical Systems (CUDOS), Laser Physics Centre, The Australian National University, Canberra, ACT 0200, Australia

bld111@rsphysse.anu.edu.au

Abstract: We demonstrate broadband wavelength conversion of a 40 Gb/s return-to-zero signal using four-wave-mixing (FWM) in a dispersion engineered chalcogenide glass waveguide. The 6 cm long planar rib waveguide 2 μm wide was fabricated in a 0.87 μm thick film etched 350nm deep to correspond to a design where waveguide dispersion offsets the material leading to near-zero dispersion in the C-band and broadband phase matched FWM. The reduced dimensions also enhance the nonlinear coefficient to 9800 $\text{W}^{-1}\text{km}^{-1}$ at 1550 nm enabling broadband conversion in a shorter device. In this work, we demonstrate 80 nm wavelength conversions with 1.65 dB of power penalty at a bit-error rate of 10^{-9} . Spectral measurements and simulations indicate extended broadband operation is possible.

©2009 Optical Society of America

OCIS codes: (130.7405) Wavelength conversion devices, (190.4380) Nonlinear optics, four-wave mixing, (190.4390) Nonlinear optics, integrated optics, (230.1150) All-optical devices

References and links

1. B. Ramamurthy and B. Mukherjee, "Wavelength conversion in WDM networking," IEEE J. Sel. Area Comm. **16**, 1061-1073 (1998).
2. G. P. Agrawal, *Nonlinear Fiber Optics* (Academic Press, San Diego, California, 2001).
3. E. Ciaramella and S. Trillo, "All-optical signal reshaping via four-wave mixing in optical fibers," IEEE Photonics Technol. Lett. **12**, 849-851 (2000).
4. H. Simos, A. Bogris, and D. Syvridis, "Investigation of a 2R all-optical regenerator based on four-wave mixing in a semiconductor optical amplifier," J. Lightwave Technol. **22**, 595-604 (2004).
5. H. Fukuda, K. Yamada, T. Shoji, M. Takahashi, T. Tsuchizawa, T. Watanabe, J.-i. Takahashi, and S.-i. Itabashi, "Four-wave mixing in silicon wire waveguides," Opt. Express **13**, 4629-4637 (2005).
6. M. Asobe, "Nonlinear optical properties of chalcogenide glass fibers and their application to all-optical switching," Opt. Fiber Technol. **3**, 142-148 (1997).
7. K. Yamada, H. Fukuda, T. Tsuchizawa, T. Watanabe, T. Shoji, and S. Itabashi, "All-optical efficient wavelength conversion using silicon photonic wire waveguide," IEEE Photonics Technol. Lett. **18**, 1046-1048 (2006).
8. V. G. Ta'eed, N. J. Baker, L. B. Fu, K. Finsterbusch, M. R. E. Lamont, D. J. Moss, H. C. Nguyen, B. J. Eggleton, D. Y. Choi, S. Madden, and B. Luther-Davies, "Ultrafast all-optical chalcogenide glass photonic circuits," Opt. Express **15**, 9205-9221 (2007).
9. V. G. Ta'eed, M. D. Pelusi, B. J. Eggleton, D. Y. Choi, S. Madden, D. Bulla, and B. Luther-Davies, "Broadband wavelength conversion at 40 Gb/s using long serpentine As₂S₃ planar waveguides," Opt. Express **15**, 15047-15052 (2007).
10. M. R. Lamont, B. Luther-Davies, D.-Y. Choi, S. Madden, X. Gai, and B. J. Eggleton, "Net-gain from a parametric amplifier on a chalcogenide optical chip," Opt. Express **16**, 20374-20381 (2008).
11. K. Inoue, "Suppression of level fluctuation without extinction ratio degradation based on output saturation in higher order optical parametric interaction in fiber," IEEE Photon. Technol. Lett. **13**, 338-340 (2001).
12. A. Bogris and D. Syvridis, "Regenerative properties of a pump-modulated four-wave mixing scheme in dispersion-shifted fibers," J. Lightwave Technol. **21**, 1892-1902 (2003).

13. R. Salem, M. A. Foster, A. C. Turner, D. F. Geraghty, M. Lipson, and A. L. Gaeta, "Signal regeneration using low-power four-wave mixing on silicon chip," *Nat. Photonics* **2**, 35-38 (2008).
14. A. W. Snyder, J. D. Love, *Optical Waveguide Theory* (Chapman & Hall November 1983)
15. M. R. E. Lamont, C. M. de Sterke, and B. J. Eggleton, "Dispersion engineering of highly nonlinear As_2S_3 waveguides for parametric gain and wavelength conversion," *Opt. Express* **15**, 9458-9463 (2007).
16. S. J. Madden, D. Y. Choi, D. A. Bulla, A. V. Rode, B. Luther-Davies, V. G. Ta'eed, M. D. Pelusi, and B. J. Eggleton, "Long, low loss etched As_2S_3 chalcogenide waveguides for all-optical signal regeneration," *Opt. Express* **15**, 14414-14421 (2007).
17. M. D. Pelusi, V. G. Ta'eed, M. R. E. Lamont, S. Madden, D. Y. Choi, B. Luther-Davies, and B. J. Eggleton, "Ultra-high Nonlinear As_2S_3 planar waveguide for 160-Gb/s optical time-division demultiplexing by four-wave mixing," *IEEE Photonics Technol. Lett.* **19**, 1496-1498 (2007).
18. M.A. Foster et al., "Broad-band continuous-wave parametric wavelength conversion in silicon nanowaveguides," *Nature* **441**, 960, (2006)
19. J. Hansryd et al. "Wavelength tunable 40 GHz pulse source based on fibre optical parametric amplifier," *Elect. Lett.* **37**, 584 (2001).
20. C. Bres, et al. "1-to-40 Channel Multicasting in Wideband Parametric Amplifier," *IEEE LEOS Winter Topicals, Sorrento Italy 1/2008*
21. J.M. Chavez Boggio et al. "730-nm optical parametric conversion from near- to short-wave infrared band," *Optics Exp.* **16**, 5435 (2008).

1. Introduction

For wavelength routed networks, wavelength conversion is necessary to avoid the wavelength continuity constraint which otherwise restricts network efficiency. All-optical wavelength conversion based on 3rd order nonlinear processes such as four-wave mixing (FWM), cross-gain modulation (XGM) or cross-phase modulation (XPM) can circumvent these limitations [1]. If the stringent phase-matching condition can be met, FWM provides a highly efficient means of achieving wavelength conversion over broad operational bandwidths. In the normal dispersion regime precise phase-matching cannot be achieved (neglecting higher-order dispersion), although FWM can still provide wavelength conversion over a narrow bandwidth. In the anomalous regime, phase-matching is possible [2], enabling broadband operation, which is a key feature for high-speed communication systems.

FWM based wavelength conversion has been demonstrated on several platforms including silica fibre [3], SOA devices [4], and silicon nanowires [5]. Chalcogenide glasses have been known as an alternative platform for nonlinear signal processing for at least a decade [6]. These glasses possess the desirable combination of strong nonlinearity (nonlinear index n_2 of As_2S_3 ~130 times greater than silica [6]), intrinsically fast response time (not limited by free carriers as in silicon [7]), and low to moderate nonlinear absorption [8]. As with silicon, chalcogenide glasses can be used for the fabrication of planar waveguides, providing a platform for the development of a photonic chip that monolithically integrates several functions and is capable of handling high data rate signals. Several of these functions have been demonstrated previously, including wavelength conversion using XPM [9]. However, chalcogenide glasses have a strong normal material dispersion at telecom wavelengths which inhibits FWM processes. Recent progress on dispersion engineered As_2S_3 chalcogenide glass waveguides has resulted in anomalous dispersion across the C-band, making FWM an ideal scheme for wavelength conversion [10], which was reported recently for low repetition rate.

In this paper, we demonstrate broadband wavelength conversion at 40 Gb/s via FWM in a 6.0 cm long dispersion-engineered As_2S_3 chalcogenide glass waveguide with a high nonlinear coefficient of ~9800 /W/km. We demonstrate wavelength conversion of a 40 Gb/s signal over an 80 nm span with just over 1.65 dB power penalty at a bit-error rate (BER) of 10^{-9} . Due its anomalous dispersion, this device can be readily reconfigured to convert C-band data into any of the telecommunication bands (S-, C- or L-bands) which covers the 1490 to 1590 nm wavelength range.

2. Principle of operation

The conventional wavelength conversion scheme, shown in Fig. 1(a), uses a continuous wave (CW) as pump. To lower the pump power requirement in this work we used another scheme, shown in Fig.1(b), where a high bit rate signal is used as the pump (at carrier frequency ω_p)

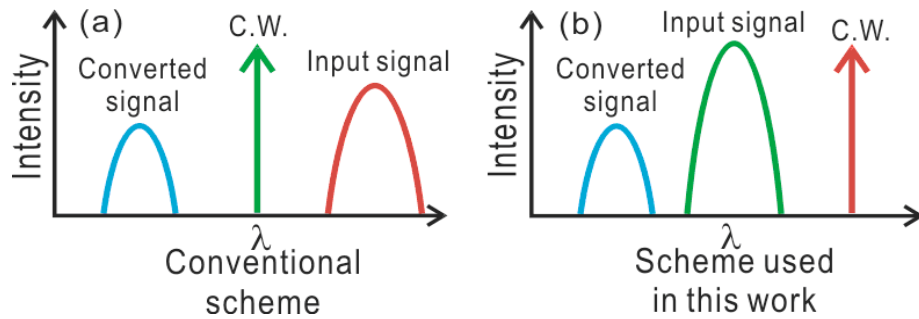


Fig. 1. Comparison of conventional wavelength conversion scheme and the scheme used in this work.

and co-propagates with a co-polarized monochromatic CW probe (of frequency ω_{cw}) in the waveguide. By filtering and isolating the idler ($\omega_i = 2\omega_p - \omega_{cw}$), data encoded in the amplitude of the pulsed pump is transferred to the idler pulses. Apart from lower pump power requirement, an added advantage of the pulsed pump wavelength converter is the potential capability of 2R regeneration [11 -13], which is important for future high bit-rate experiments.

The gain experienced by the CW signal and converted signal is characterized by the exponential coefficient $g = [-\Delta\beta (\Delta\beta + 2\gamma P)]^{1/2}$, where $\Delta\beta = \beta_2(\omega_i - \omega_p)^2/2$ is the dispersive-phase mismatch (assuming higher order dispersion has a negligible contribution); β_2 is the second-order dispersion coefficient at the pump wavelength; P is the peak power of the pump; and γ is the nonlinear coefficient. For exponential gain to occur near ω_p , g must be real and thus β_2 must be negative, or the group-velocity dispersion GVD must be positive (i.e. the dispersion is anomalous) [2]. The material dispersion of As_2S_3 chalcogenide glass is large and normal and at a wavelength of 1550 nm, $D_{mat} \sim -360$ ps/nm/km. However, the GVD experienced by a propagating mode is a combination of the dispersion due to the material with that due to the geometry of the waveguide (D_{wg}) [14], i.e. $GVD = D_{mat} + D_{wg}$. Reducing the transverse dimensions of the waveguide (height and width) results in an increasing anomalous D_{wg} [15], thus the GVD can be engineered to a specific value. For wavelength conversion, a small and anomalous dispersion is required for efficient and broadband FWM.

A diagram of the engineered As_2S_3 waveguide and its dispersion is shown in Fig. 2. The dispersion for the fundamental TE and TM modes was calculated using a finite element method (RSoft FemSIMTM) and shows that the dispersion of the fundamental TE (horizontally polarized) mode remains normal, while the dispersion of the TM (vertically polarized) mode is small and anomalous within the C-band [15].

3. Experimental results

The fabrication of the As_2S_3 waveguide is described in [16] and involved thermally depositing a 870 nm thick film of As_2S_3 ($n \approx 2.4$) on a 100mm diameter oxidized silicon wafer ($n = 1.44$).

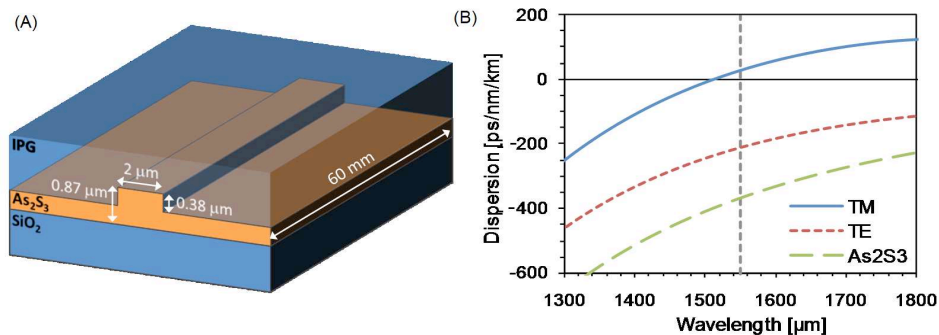


Fig. 2. (a) The schematic plot of the waveguide and (b) the calculated group velocity dispersion of fundamental TM and TE mode (right).

From this, 6 cm long ribs of 2 μm width were formed by photolithography and dry-etching surrounding trenches 350 nm deep. The chip was then over-clad with a polymer layer ($n=1.51$). Mode solving with the waveguide parameters gave an effective mode area of approximately 1.23 μm^2 , corresponding to a nonlinear coefficient of $\sim 9800 \text{ /W/km}$ and a total dispersion of $\sim 29.2 \text{ ps/nm/km}$ for the TM mode. Lensed fibres with 2.5 μm mode field diameter were used for input and output coupling to the waveguide. The total insertion loss (including the mode mismatch, index mismatch at both facets, and propagations loss of $\sim 1 \text{ dB/cm}$) was 15.5 dB for TM mode and 14.0 dB for TE mode. The insertion loss of these waveguides is higher than our previous reported results [9] due to the reduced waveguide thickness, associated with the dispersion engineering [10].

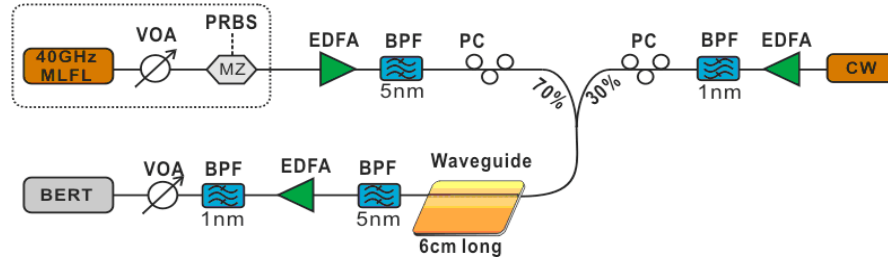


Fig. 3. Experimental setup for wavelength conversion by FWM.

Figure 3 shows the experimental setup used. The signal (pump) was generated from an optically filtered 40 GHz actively mode-locked fibre laser (MLFL) producing a 2 ps pulse train. An external electro-optic Mach-Zehnder (MZ) modulator encoded a pseudorandom sequence (PRBS) of length $2^{31}-1$ bits generated from a 40 Gb/s pattern generator. The pulse train was amplified using a high-power erbium-doped fibre amplifier (EDFA) and passed through a 5 nm band-pass filter (BPF) to remove the ASE noise background. A 70/30 coupler combined the signal (70%) with a CW probe (30%) that was generated from an amplified external-cavity diode-laser and filtered with a 1 nm BPF. The polarization of both the pump and probe were controlled to allow alignment to the TM mode of the waveguide, which has anomalous dispersion, and to maximize the conversion efficiency. Coupling into the TM and TE modes was distinguished by observing the differential group delay on an optical sampling scope; the group velocity of the TM mode is slower than that of the TE mode throughout the C-band.

Figure 4 shows the output spectra from the waveguide for the signal fixed at either at 1535 or 1560 nm, while the CW probe was scanned across the C-band. The total launch power was kept at 102 mW corresponding to an optical power coupled into the waveguide of 33.0 mW for the signal, and 10.0 mW for the probe (assuming 3.75 dB/facet coupling loss). It shows for an arbitrary wavelength of the CW probe (limited by the gain bandwidth of the EDFA) that an idler was generated with near uniform efficiency, highlighting that broadband phase matching was achieved. With the signal at 1535 nm (Fig. 4(a)), the idler was generated in the S-band down to near 1490 nm. With the signal at 1560 nm (Fig. 4(b)), conversion to the L-band near 1590 nm was achieved. The experimental spectra showed a close fit to the numerical simulations obtained using the Split Step Fourier Method (SSFM) [2] for the same waveguide and experiment parameters. The simulated gain envelope of the converted signal has a 3 dB-bandwidth over 80 nm. This is much larger than previous wavelength conversion results demonstrated using XPM in a waveguide with large normal dispersion [9]. When the pump is at 1535 nm (Fig. 4(a)) the performance is slightly better than in the case of 1560 nm (Fig. 4(b)). This is due to the absolute value of dispersion at 1560 nm ($\beta_2 \sim -46 \text{ ps}^2/\text{km}$), which is higher than that at 1535 nm ($\beta_2 \sim -24 \text{ ps}^2/\text{km}$).

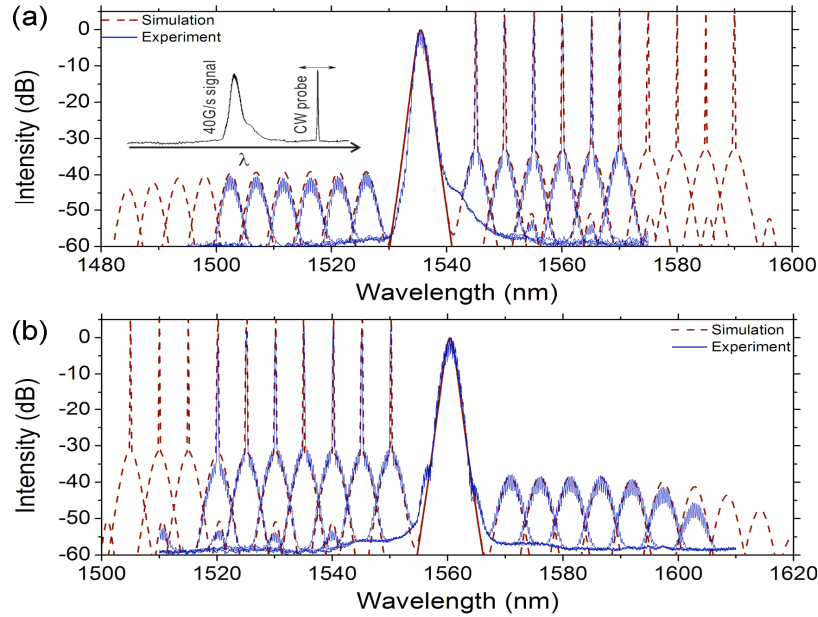


Fig. 4. Measured optical spectra after propagation through the As_2S_3 waveguide for the 40Gb/s input data pulses centered at (a) 1535 nm and (b) 1560 nm, with the wavelength offset of the CW probe varied. The solid blue line represents the experimental data, while the dashed red lines represent simulations using the SSFM. The inset shows an example spectrum at input.

Bit error rate testing (BERT) of the converted data was carried out with the input 40 Gb/s signal at 1550 nm and the CW probe at 1570 nm. The wavelength converted signal at 1530 nm was filtered with a 5 nm BPF and directed to the receiver consisting of a low-noise EDFA, 1.0 nm BPF, variable optical attenuator (VOA) and 40 GHz photo-detector (PD). The MLFL, pattern generator and receiver were synchronized using an external 40 Gb/s RF clock. The

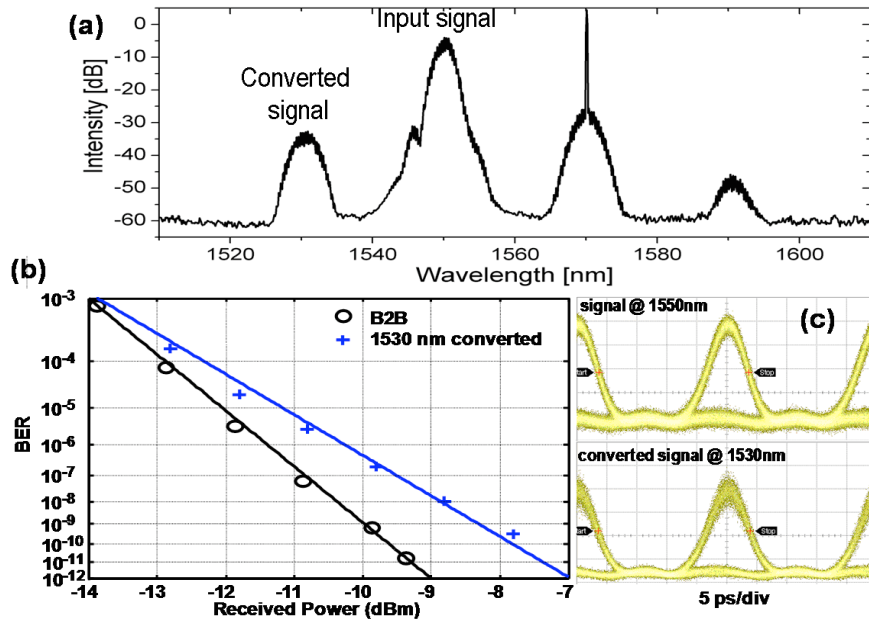


Fig. 5. (a) Output spectrum at the output of the waveguide. (b): BER versus received optical power for back-to-back (B2B) and converted signals. (c): Data eye diagram (65GHz optical bandwidth detector) for 40 Gb/s back-to-back input (B2B) and wavelength converted signals

average power of the 40 Gb/s signal at the input connector of the waveguide was 21.5 dBm for the signal 19.2 dBm for the probe for a total of 23.5 dBm (224 mW). The power coupled into the As_2S_3 waveguide was ~ 19.7 dBm (93 mW). The peak power of the input signal is about 730 mW inside the waveguide. Figure 5(a) shows the spectrum at the output of the waveguide. The measured bit error rates (BER) for varying received power are shown in Fig. 5(b). At a BER of 10^{-9} , there is 1.65 dB power penalty for the converted signal compared to the original 40 Gb/s signal compared with the back to back (B2B) measurements (the signal taken directly from the MZ modulator to the VOA then to the photodetector). The power penalty is mainly due to the noise from the amplifiers and small power fluctuations of the CW probe due to the weak Fabry-Pérot effects from the facets of the waveguide.

4. Discussion and conclusion

The benefit of dispersion engineering for FWM is demonstrated in Fig. 6, which shows a comparison between the simulated FWM conversion efficiency for the As_2S_3 waveguide with and without dispersion engineering. The FWM efficiency is defined as the ratio of the output peak power of the idler pulse to the input peak power of the probe (CW is our case). In Fig. 6, SSFM simulations were used to calculate this efficiency as a function of idler wavelength detuning for two different waveguides: the waveguide used in this experiment and the waveguide used in a previous FWM-based experiment [17]. In both cases, the pump was centred at 1530 nm and the peak power was scaled so that the peak intensities inside the waveguides were the same. In the previous experiment [9], an As_2S_3 waveguide without dispersion engineering (β_2 of 435 ps²/nm) was used for wavelength conversion. The FWM bandwidth was very limited (the red dashed curve in Fig. 6) and broad-band operation could only be achieved using XPM, which is difficult to implement in reality due to the strong CW component in the converted signal. The dispersion-engineered waveguide, on the other hand, maintains constant conversion efficiency over a very broad wavelength range (the black solid curve in Fig. 6), making it ideal for wavelength conversion. In Fig. 6, when close to the pump wavelength there is notable difference of the FWM efficiency between the two types of waveguides. This is due to the difference in propagation loss. For the waveguide without dispersion engineering, the propagation loss is around 0.05 dB/cm whereas the dispersion engineered waveguide (the one used in this experiment) has a propagation loss of around 1.0 dB/cm. So a significant improvement of the FWM efficiency and much lower power consumption is expected if the propagation loss is reduced, which we are addressing.

In conclusion, we have demonstrated 40 G/s wavelength conversion using dispersion engineered chalcogenide planar waveguide and achieved broadband operation. The converted

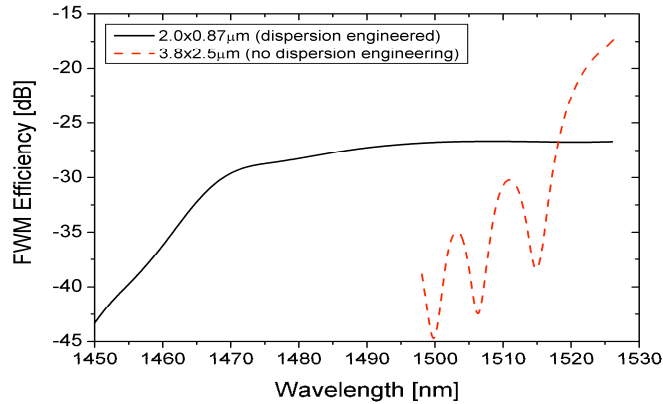


Fig. 6. Simulated comparison of the wavelength conversion efficiency of the dispersion engineered waveguide (with anomalous dispersion, solid line) to the As_2S_3 waveguide used in previous FWM experiments [9] (with normal dispersion, dashed line). The pump is centred at a wavelength of 1530 nm and the peak power is scaled (0.35 W and 1.62 W) such that the peak intensities are the same in both cases, although the propagation losses differ.

signal was error free and has 1.65 dB power penalty. This device can be readily reconfigured to convert C-band data into any of the telecommunication bands (S-, C- or L-bands) which covers the 1490 to 1590 nm wavelength range. Together with other reported platforms [3-5, 18-21], the dispersion engineered As_2S_3 waveguides (possessing ultra-fast nonlinearity and broadband operation capability) is a good candidate for ultra-high bandwidth optical signal processing. For our future work we will concentrate on lowering the insertion losses and making longer waveguides, which will reduce the power consumption and increase the conversion efficiency.

Acknowledgments

Funding from the Australian Research Council (ARC) through its Federation Fellow and Centres of Excellence programs is gratefully acknowledged. The Centre for Ultrahigh-bandwidth Devices for Optical Systems (CUDOS) is an ARC Centre of Excellence.